Electronic Supporting Information for:

Halogen bonding modulates hydrogel formation from Fmoc amino acids

A. Pizzi,[a] L. Lascialfari,[a] N. Demitri,[b] A. Bertolani,[a] D. Maiolo,[a] E. Carretti[d] and P. Metrangolo[a,c]

a) Laboratory of Nanostructured Fluorinated Materials (NFMLab), Department of Chemistry, Materials and Chemical Engineering "Giulio Natta", Politecnico di Milano, Via L. Mancinelli 7, I-20131 Milano, Italy.

b) Elettra-Synchrotron Light Source, S.S. 14 Km 163.5, Area Science Park, 34149 Basovizza, Trieste, Italy.

c) Department of Applied Physics, Aalto University, PO Box 15100, Espoo FI-02150, Finland.

d) Department of Chemistry "Ugo Schiff", Università di Firenze, Firenze, Italy

General Remarks

Reagents.

All the reagents were purchased from Sigma-Aldrich, and used without any further purification.

Experimental Techniques

TEM. TEM bright field images were acquired using a Philips CM200 electron microscope operating at 200 kV equipped with a Field Emission Gun filament. A Gatan US 1000 CCD camera was used and 2048x2048 pixels images with 256 grey levels were recorded. The suspension were dropped onto a 200 mesh carbon-coated copper grid and air dried for several hours before analysis.

Rheology. All rheology tests were performed using a Physica-Paar UDS 200 rheometer, equipped with a plate–plate geometry measuring system (diameter of the upper plate 4.0 cm, measuring gap: 500 μm). Temperature was controlled with a Peltier device and maintained at 25°C. All the oscillatory measurements were performed within the linear viscoelastic range of gels that has been determined by means of Strain Sweep tests (Figure 2S_A) collected by maintaining the oscillation frequency constantly equal to 1 Hz.. The instrumental setups for the rheology tests are the following: Frequency sweep test: frequency range 100 Hz to 0.001 Hz; strain 1%. All the measurements were repeated a minimum of three times.

Fibrillation kinetics. Measurements were performed on a Tecan GENios plate reader employing as a sample holder a full transparent 96 wellplate. The instrument was set at 25 °C and orbital shaking was set at 700–1100 revolutions per minute (rpm). Each well was filled with 150 μL of the proper Fmoc-4-X-Phe solution. Each sample was measured in triplicate. Method: (i) shaking 30 s; (ii) wait 150 s; (iii) shake 2 s; (iv) measure absorption at 405 nm; (v) repeat stages ii-iv for 16

hours. Each sample was subtracted with the blank solution, i.e. 5% DMSO in PBS Buffer solution (pH = 7.4). Each measurement was fitted accordingly to equation 1 (Verhulst logistic function):[1S]

$$Y = y_i \frac{y_f}{1 + e^{-(t-t_0)/\tau}} \qquad \text{(eq. 1)}$$

Where: Y = absorbance, being y_i and y_f the initial and final absorbance values respectively;

t_0 = time to 50% of maximal signal or the time of inflection point;

τ = time constant of fibril growth

From the fitting two parameter can be extrapolated to figure out the fibril growth process:

$k_{app} = 1/\tau$ apparent growth rate of fibrils

$T = t_0 - 2\tau$ delay time

Higher is the k_{app}, faster is the fibrillation, while higher is the delay time, slower is the kinetic fibrillation.

Gelation experiments. Hydrogels were prepared in small (1 mL) capped vials by adding PBS buffer (pH = 7.4) to a proper volume of a DMSO stock solution of the amino acid to reach the desired concentration and the desired percentage of DMSO in the final mixture. The resulting suspensions (upon addition of PBS to the DMSO stock solution, the amino acid precipitates), was vortexed 30 s at 20x100 rpm, and heated using a heat gun until complete dissolution. The resulting solution were allowed to cool at r.t. and tested for the gel formation through the "test-tube inversion".[2S].

Thermal stability. The vials containing the hydrogels at 5 mM or 1 mM concentration were inverted and fixed at the bottom of an oil bath with stirring. The temperature was kept at 25 °C for 10 min to equilibrate the system and then gradually increased from 25 to 120 °C (at 1 °C min^{-1}). The range temperature within the gels break and fall down is regarded as melting point range.

Crystallization assays. Fmoc-4-F-Phe crystals were obtained by dissolving the compound in a mixture DMSO/water 95:5. Crystals suitable for XRD analysis formed after 1 month of slow evaporation at room temperature. Fmoc-4-Cl-Phe crystals were obtained by dissolving the compound in N-methyl acetamide. Crystals suitable for XRD analysis formed after 1 month of slow evaporation at 45 °C. Fmoc-4-Br-Phe crystals were obtained by dissolving the compound in a mixture hexafluoro-2-propanol/water 95:5. Crystals suitable for XRD analysis formed after 1 month of slow evaporation at room temperature. Fmoc-4-I-Phe crystals were obtained by dissolving the compound in a mixture

dichloromethane/hexafluoro-2-propanol 1:1. Crystals suitable for XRD analysis formed after 1 month of slow evaporation at room temperature. Data collections were performed at the X-ray diffraction beamline (XRD1) of the Elettra Synchrotron, Trieste (Italy) – beam time provided through proposals with numbers 20150542 and 20155517.

Figures

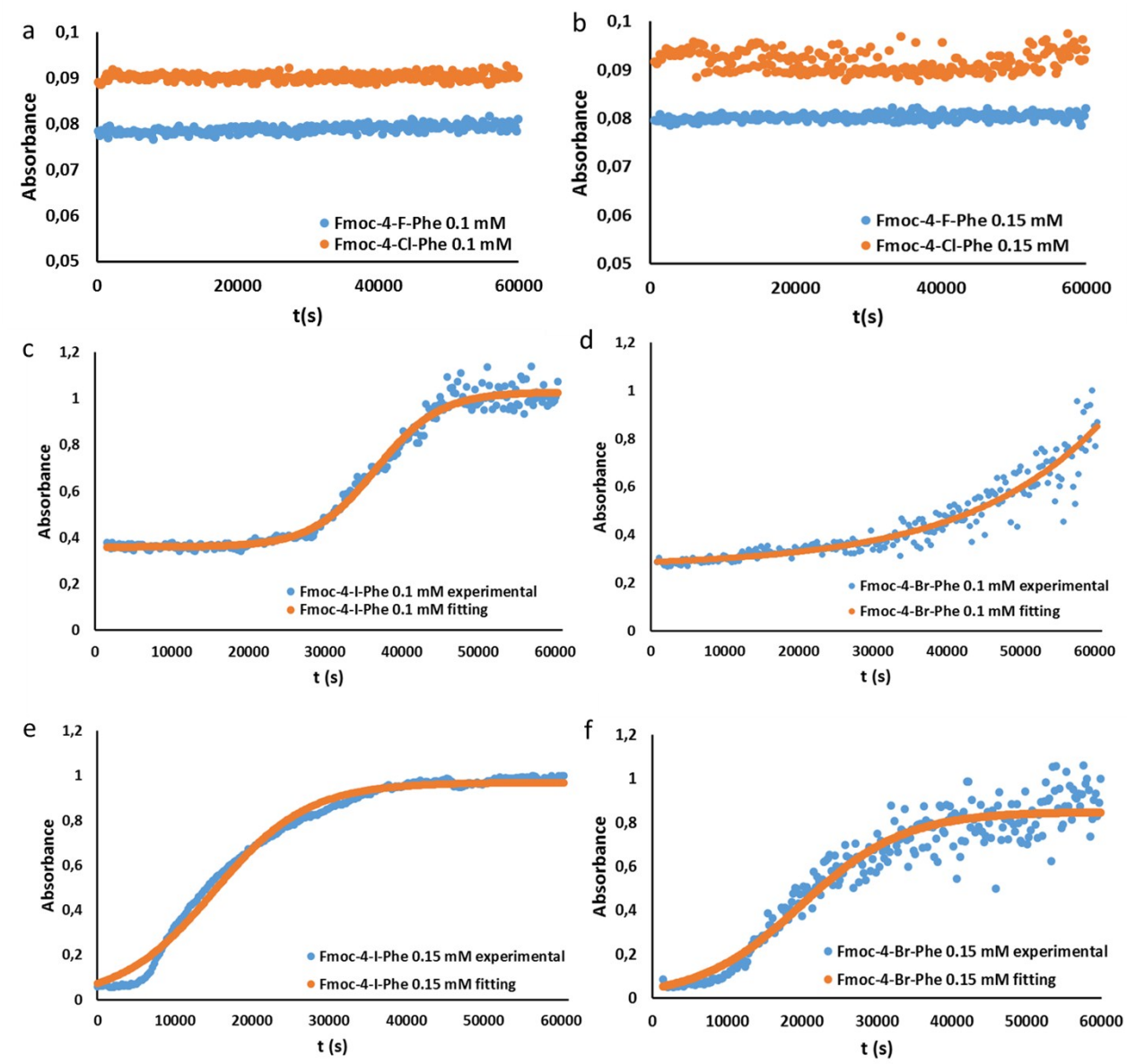

Figure 1S. Fibrillation Kinetics at 25 °C of Fmoc-4-X-Phe. Fluorinated and chlorinated amino acids at 0.1 mM concentration (a) do not an increased solution scattering typical of fibrillation process. Increasing the concentration (b) has no effect on the kinetic. Fmoc-4-I-Phe 0.1 mM kinetics (c) follows the expected trend. Fmoc-4-Br-Phe 0.1 mM kinetics (d) is still in the growing phase in the considered time interval. Increasing the concentration of Fmoc-4-I-Phe leads to a faster kinetic (e). Increasing the concentration of Fmoc-4-Br-Phe leads the fibrillation process to completeness.

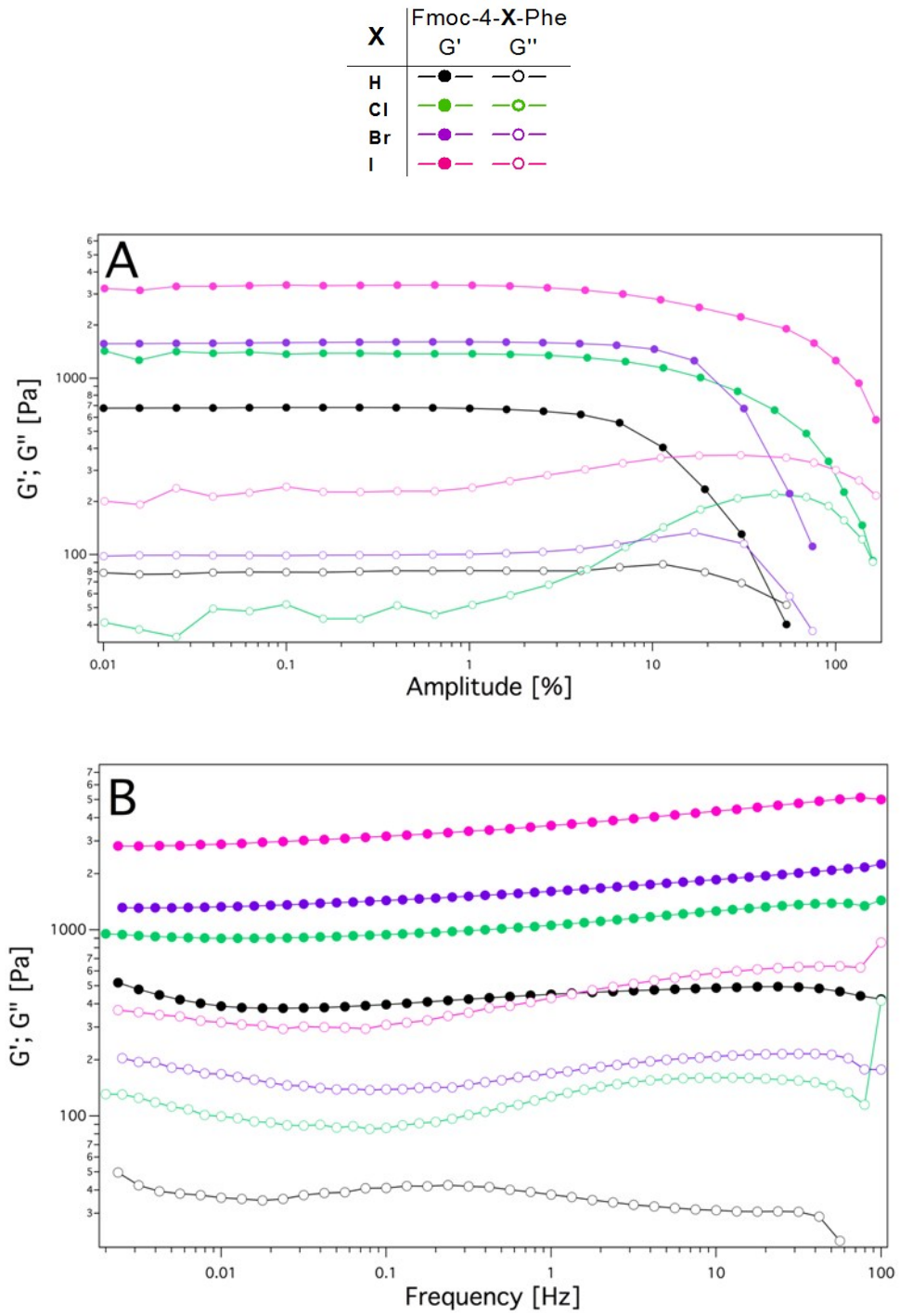

Figure 2S. A) Strain Sweeps and B) Frequency Sweeps of Fmoc-4-X-Phe 5 mM gel samples in 5 % DMSO/PBS". The measurements are performed in the linear viscoelastic range of the gels. G' values are systematically higher than G'', confirming that the observed samples were true gels. The gels were quite robust; in particular, the gel formed by the iodinated amino acid (X=I) was the stiffest of the series. It was not possible to obtain reliable and reproducible measurements on the gel of the fluorinated derivative, as it formed only a very weak gel.

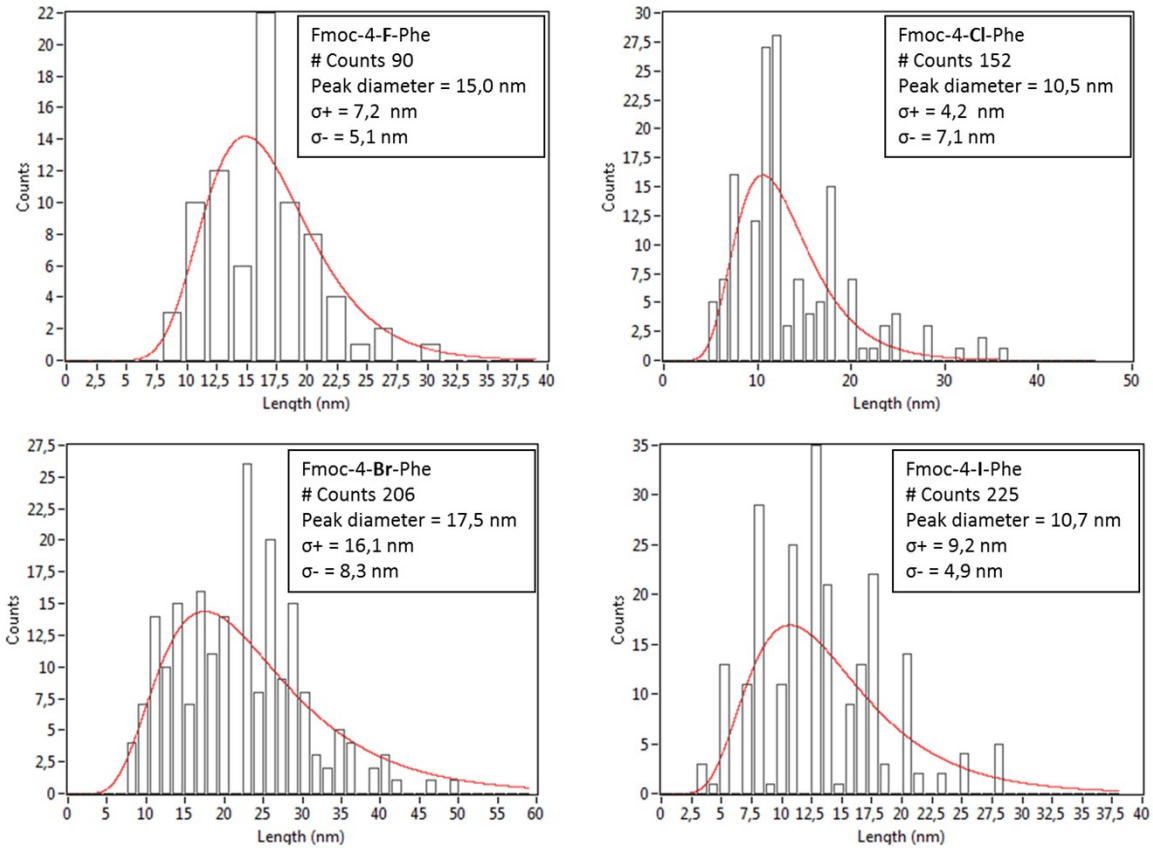

Figure 3S. Statistical analysis of diameter of fibers observed in the TEM micrographs of 1 mM gel sample of Fmoc-4-X-Phe in 5% DMSO/PBS. The analysis was performed with an home-made routine programs (NPStat) that has already been used in the statistical analysis of dimension of nanostructured materials observed by TEM.[3S] The analysis shows that the dimension of fibers is similar amongst the different sample, being the bromo derivative the one giving the slightly bigger and less monodisperse diameter range.

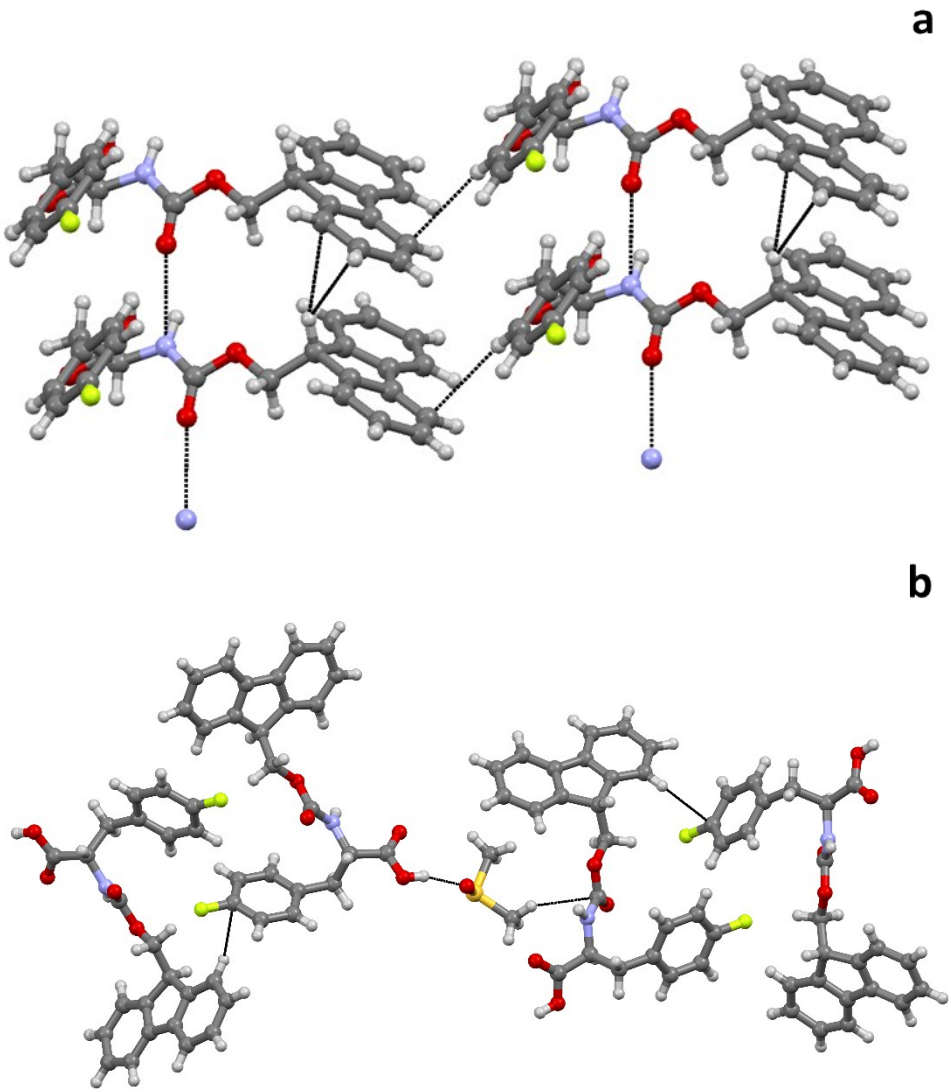

Figure 4S. Crystal structure of Fmoc-4-F-Phe. Fmoc-4F-Phe crystallizes in the $P2_12_12_1$ space group. The asymmetric unit consists of a single molecule of amino acid solvated by one disordered molecule of DMSO. a) The crystal structure grows along the *a* crystallographic axis through strong hydrogen bond contacts N···O between the carbonyl group of the Fmoc moiety and the nitrogen of an adjacent amino acid molecule, forming an infinite chain (Table 1bS). The crystal packing is further stabilized by C–H···π interactions between the Fmoc moieties. b) Along the crystallographic axis *c* the structure grows through C–H···π contacts between the Fmoc moiety and the phenyl ring of a near molecule. Along the same direction, DMSO molecules join independent chains through intermolecular hydrogen bonding and short contacts C···H.

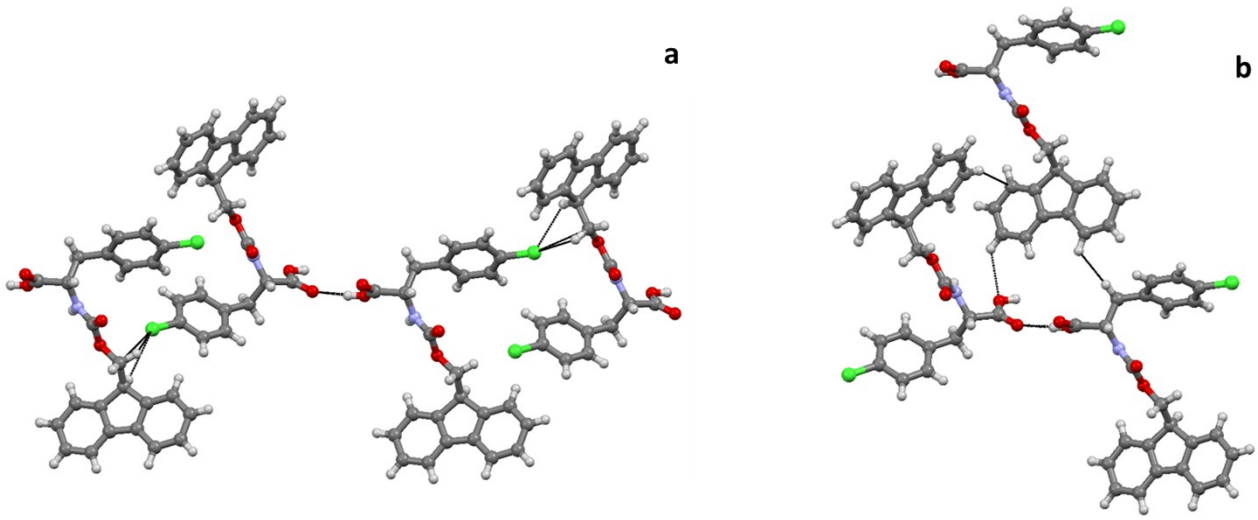

Figure 5S. Crystal structure of Fmoc-4-Cl-Phe. Fmoc-4Cl-Phe crystallizes in the $P2_1$ space group. The asymmetric unit consists of a single molecule of amino acid. a) Chlorine shows short contacts Cl···C and Cl···H with the methylene group of the Fmoc moiety of a neighboring amino acid molecule (C···Cl distance 3.37(1) Å). A hydrogen bond network between peptidic groups of neighbour molecule characterize crystal packing along crystallographic *b* axis (Table 1bS). b) Along the crystallographic axis *c* the structure grows through C–H···π contacts between the Fmoc moieties of adjacent molecules. In this direction, intermolecular short contacts H···H and C–H···O stabilize the crystal packing.

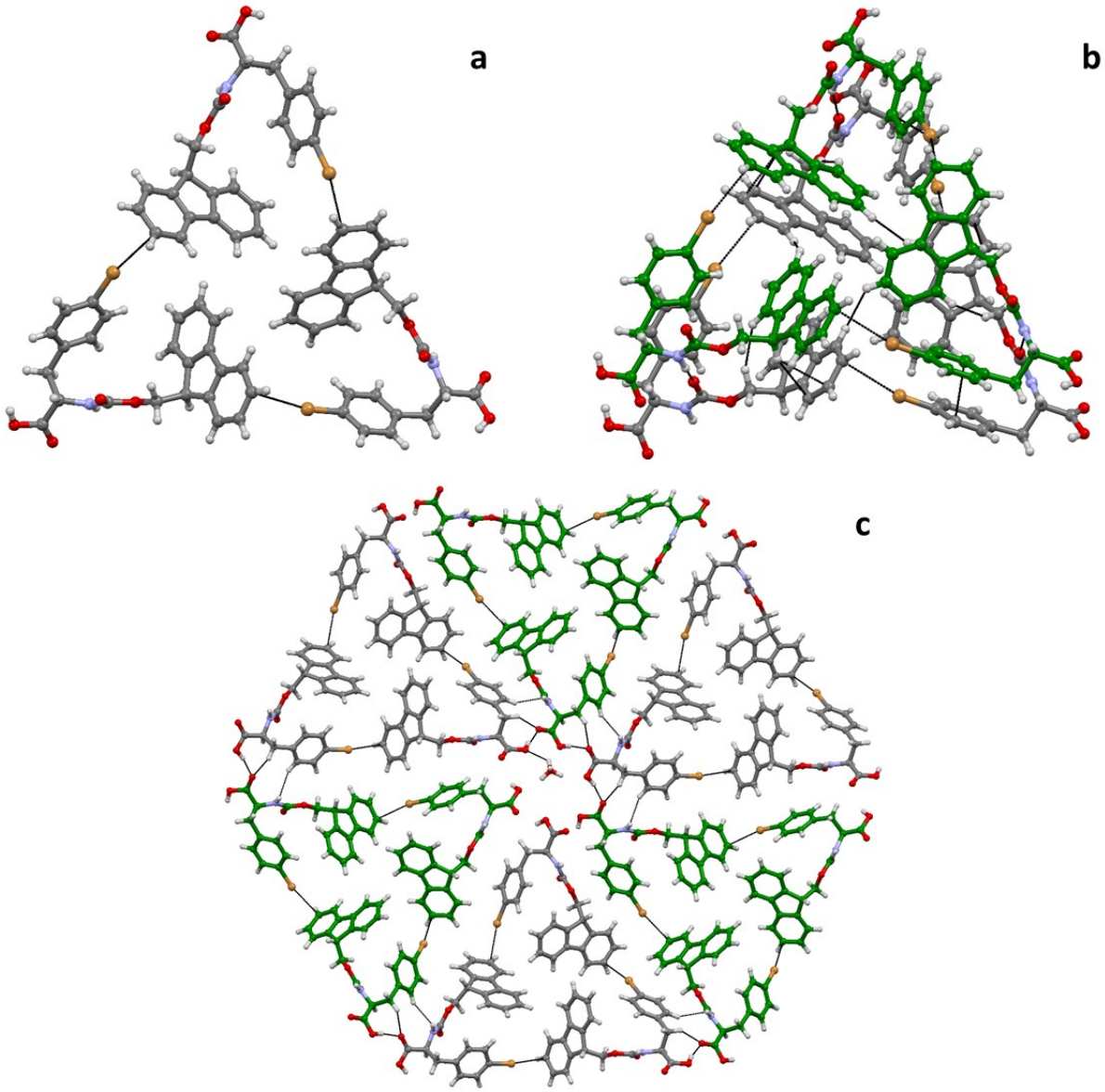

Figure 6S. Crystal structure of Fmoc-4-Br-Phe. Fmoc-4Br-Phe crystallizes in the $P6_3$ space group. The asymmetric unit consists of a single molecule of amino acid solvated by water molecules. a) Bromine interacts with the Fmoc moiety of a neighboring amino acid molecule (Br···π distance 3.76 Å), resulting in a compact repeating unit formed by three molecules of Fmoc-4Br-Phe, with C_3 symmetry. b) These units stacks along the *c* crystallographic axis through N–H···O hydrogen bonds between the carbonyl group of the Fmoc moiety and the N–H group of an adjacent amino acid molecule lying on another plane (Table 1bS). Along this direction, the crystal packing is further stabilized by intermolecular short contacts H···H, π···π (among phenyl rings) and C–H···π (among Fmoc moieties). c) The crystal structure grows along both the crystallographic axis *a* and *b* via hydrogen bonding between the C-terminal groups of neighboring molecules, belonging to independent three-membered units, creating narrow channels filled by tightly coordinated water molecules.

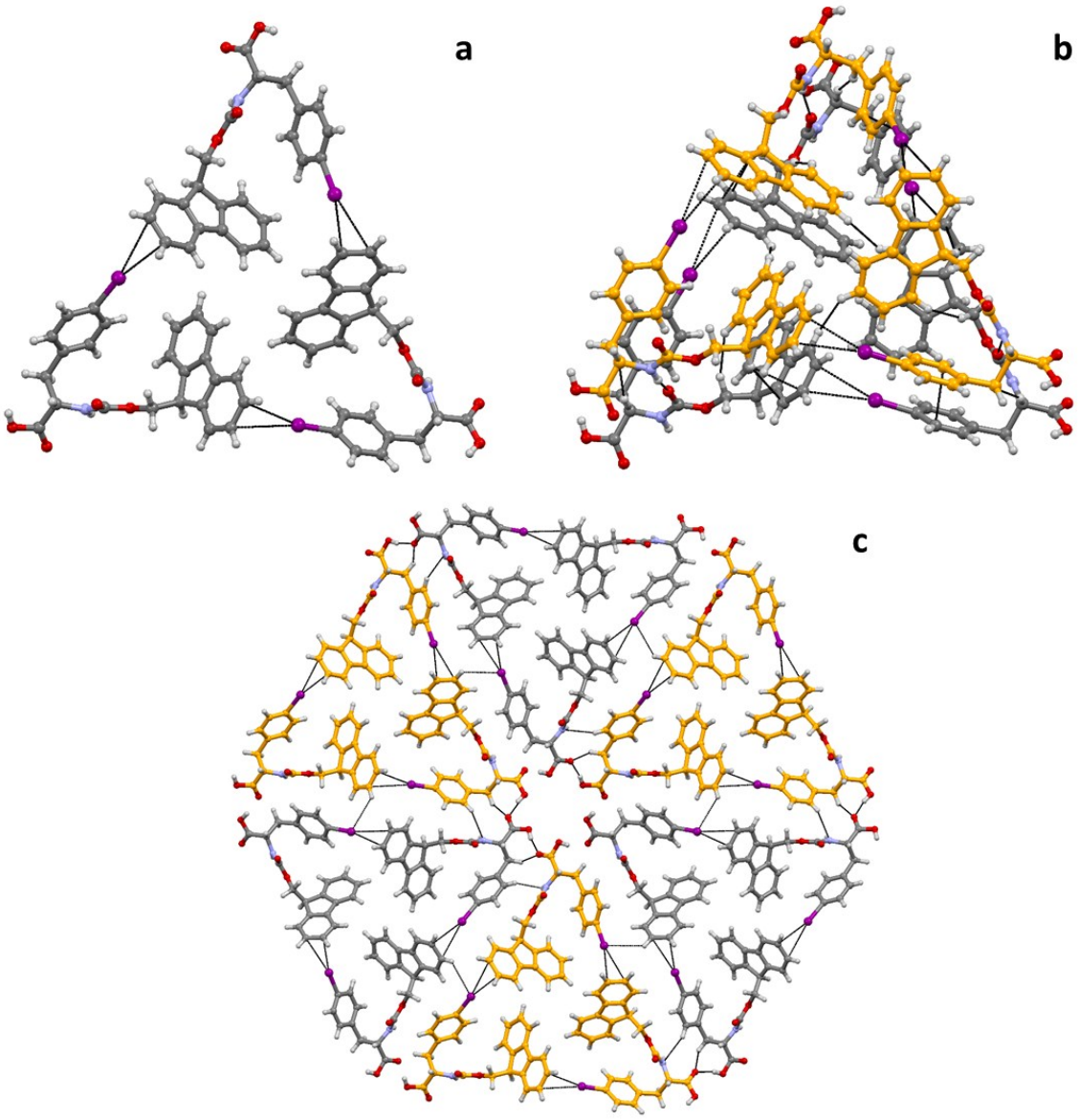

Figure 7S. Crystal structure of Fmoc-4-I-Phe. Fmoc-4I-Phe crystallizes in the $P6_3$ space group. The asymmetric unit consists of a single molecule of amino acid solvated by water molecules. a) Iodine interacts with the Fmoc moiety of a neighboring amino acid molecule (I···π distance ~3.83 Å), resulting in a compact repeating unit formed by three molecules of Fmoc-4I-Phe, with C_3 symmetry. b) These units stacks along the *c* crystallographic axis through N–H···O hydrogen bonds between the carbonyl group of the Fmoc moiety and the N–H group of an adjacent amino acid molecule lying on another plane. Along this direction, the crystal packing is further stabilized by intermolecular short contacts H···H, π···π (among phenyl rings) and C–H···π (among Fmoc moieties). c) The crystal structure grows along both the crystallographic axis *a* and *b* via hydrogen bonding between the C-terminal groups of neighboring molecules, belonging to independent three-membered units, creating narrow channels filled by tightly coordinated water molecules.

X-ray diffraction analysis - Structural characterization of Fmoc-4-X-Phe.

Data collections were performed at the X-ray diffraction beamline (XRD1) of the Elettra Synchrotron, Trieste (Italy)[4S]. The crystals were dipped in perfluoropolyether vacuum oil (Fomblin) and mounted on the goniometer head with a nylon loop. Complete datasets were collected at 100 K (nitrogen stream supplied through an Oxford Cryostream 700) through the rotating crystal method. Data were acquired using a monochromatic wavelength of 0.700 Å for **Fmoc-4-Cl-Phe**, **Fmoc-4-Br-Phe**, **Fmoc-4-I-Phe** and 0.800 Å for **Fmoc-4-F-Phe**, on a Pilatus 2M hybrid-pixel area detector. The diffraction data were indexed and integrated using XDS.[5S] Scaling have been done using CCP4-Aimless code.[6S, 7S] Crystals appear as very thin colorless needles or plates prone to radiation damage, as previously reported for other halogenated molecules.[8S, 9S] None of the crystals tested diffracted better than 0.85 Å, with an average dataset resolution of ~0.9 Å. For the brominated aminoacid two different datasets, collected from different crystals randomly oriented, have been merged. The structures were solved by the dual space algorithm implemented in the SHELXT code.[10S] Fourier analysis and refinement were performed by the full-matrix least-squares methods based on F^2 implemented in SHELXL (Version 2016/6)[11S]. The Coot program was used for modeling.[12S] Anisotropic thermal motion refinement have been used for all atoms with full occupancy and disordered DMSO sulphur atom in **Fmoc-4-F-Phe**. Geometric and thermal motion parameters restrains (DFIX, DANG, SIMU or DELU) have been applied on disordered and poorly defined fragments. Hydrogen atoms were included at calculated positions with isotropic $U_{factors} = 1.2\ U_{eq}$ or Ufactors = 1.5 Ueq for hydroxyl groups (Ueq being the equivalent isotropic thermal factor of the bonded non hydrogen atom). Hydrogen atoms for water molecules have not been included in the refined models of **Fmoc-4-Br-Phe** and **Fmoc-4-I-Phe** since it was not possible to locate them unambiguously in electron-density peaks of Fourier difference maps (contributions of these missing H atoms is still included in the properties reported in Table 1S).

The four aminoacids crystallize in chiral space groups with one molecule in the asymmetric unit (ASU; Figure 8S). Refined Flack parameters[13S] (Table 1S) have quite high e.s.d.s, especially for fluorine derivative, as a consequence of crystals radiation damage but are in agreement with expected phenylalanine Cα configuration.

Crystal packing of all the halogenated aminoacids show stacked molecules with strong hydrogen bonds involving neighbor peptide bonds and terminal protonated carboxylic groups. Furthermore, π-π stacking interactions keeps Fmoc and phenylalanine aromatic rings significantly overlapped (Figure 4S-7S).

Fluorine amino acid shows an orthorhombic unit cell that traps a disordered DMSO solvent molecules inside channels parallel to crystallographic *a* axis. Bromine and iodine molecules show the same hexagonal crystal packing, trapping water molecules in channels aligned with crystallographic

c axis. The water molecules lie on and adjacent to crystallographic 6_3 screw axis and keep tightly connected hexamer of molecules exposing their carboxylic groups in the channels. Cell volume is slightly bigger for the iodinated peptide, as expected from comparison of halogens atomic radius. Pictures were prepared using Ortep3[14S] and CCDC Mercury[15S] software. Essential crystal and refinement data (Table 1S) are reported below. CCDC 1521993-1521996 contain the supplementary crystallographic data for compounds **Fmoc-4-I-Phe**, **Fmoc-4-Br-Phe**, **Fmoc-4-F-Phe** and **Fmoc-4-Cl-Phe**. These data can be obtained free of charge from The Cambridge Crystallographic Data Centre via https://www.ccdc.cam.ac.uk/structures.

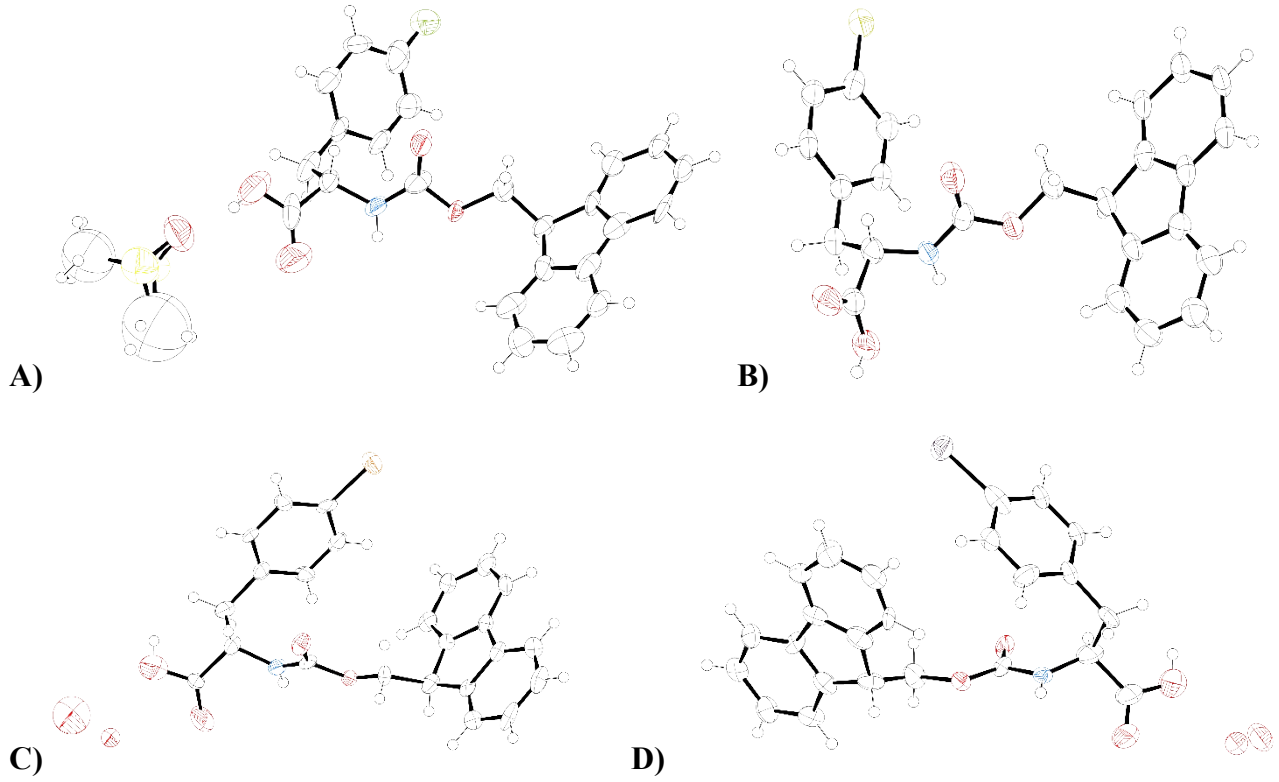

Figure 8S. Ellipsoids representation of ASU contents (50% probability) for: A) **Fmoc-4-F-Phe**, B) **Fmoc-4-Cl-Phe**, C) **Fmoc-4-Br-Phe** and D) **Fmoc-4-I-Phe**.

Tables

Table 1S. Crystallographic data and refinement details for compounds **Fmoc-4-F-Phe**, **Fmoc-4-Cl-Phe**, **Fmoc-4-Br-Phe** and **Fmoc-4-I-Phe**.

	Fmoc-4-F-Phe·C_2H_6SO [$C_{24}H_{20}FNO_4 \cdot C_2H_6SO$]	**Fmoc-4-Cl-Phe** [$C_{24}H_{20}ClNO_4$]	**Fmoc-4-Br-Phe**·⅓H_2O [$C_{24}H_{20}BrNO_4 \cdot ⅓H_2O$]	**Fmoc-4-I-Phe**·⅓H_2O [$C_{24}H_{20}INO_4 \cdot ⅓H_2O$]
CCDC Number	1521995	1521996	1521994	1521993
Chemical Formula	$C_{26}H_{26}FNO_5S$	$C_{26}H_{26}FNO_5S$	$C_{24}H_{20.67}BrNO_{4.33}$	$C_{24}H_{20.67}INO_{4.33}$
Formula weight (g/mol)	483.54	421.86	472.32	519.31
Temperature (K)	100(2)	100(2)	100(2)	100(2)
Wavelength (Å)	0.800	0.700	0.700	0.700
Crystal system	Orthorhombic	Monoclinic	Hexagonal	Hexagonal
Space Group	$P\,2_12_12_1$	$P\,2_1$	$P\,6_3$	$P\,6_3$
Unit cell dimensions	a = 4.920(1) Å	a = 13.168(3) Å	a = 26.744(4) Å	a = 26.878(4) Å
	b = 13.034(3) Å	b = 4.839(1) Å	b = 26.744(4) Å	b = 26.878(4) Å
	c = 36.789(7) Å	c = 17.400(4) Å	c = 4.997(1) Å	c = 4.999(1) Å
	α = 90°	α = 90°	α = 90°	α = 90°
	β = 90°	β = 111.41(3)°	β = 90°	β = 90°
	γ = 90°	γ = 90°	γ = 120°	γ = 120°
Volume (Å^3)	2359.2(8)	1032.2(4)	3095.2(11)	3127.6(11)
Z	4	2	6	6
Density (calculated) (g·cm^{-3})	1.361	1.357	1.520	1.654
Absorption coefficient (mm^{-1})	0.246	0.205	1.893	1.458
F(000)	1016	440	1448	1556
Crystal size (mm^3)	0.09 x 0.01 x 0.01	0.10 x 0.05 x 0.02	0.05 x 0.05 x 0.02	0.09 x 0.01 x 0.01
Crystal habit	Colorless thin needles	Colorless thin needles	Colorless thin plates	Colorless thin needles
Theta range for data collection	1.63° to 21.61°	1.24° to 24.31°	1.50° to 22.86°	1.49° to 21.61°
Index ranges	$0 \le h \le 5$	$-15 \le h \le 15$	$-25 \le h \le 25$	$-26 \le h \le 13$
	$0 \le k \le 14$	$-5 \le k \le 5$	$-25 \le k \le 25$	$-25 \le k \le 28$
	$0 \le l \le 40$	$-20 \le l \le 20$	$-5 \le l \le 3$	$-5 \le l \le 3$
Reflections collected	5409	5367	4309	4718
Independent reflections (data with I>2σ(I))	1905 (1363)	3196 (2068)	2529 (1639)	2162 (1263)
Data multiplicity (max resltn)	2.71 (2.67)	2.68 (2.94)	2.57 (2.34)	3.22 (3.32)
I/σ(I) (max resltn)	8.01 (1.74)	10.30 (1.88)	7.85 (1.61)	4.99 (2.57)
R_{merge} (max resltn)	0.0784 (0.4584)	0.0740 (0.4376)	0.1128 (0.4091)	0.1545 (0.3791)
Data completeness (max resltn)	96.4% (93.3%)	97.3% (100.0%)	98.3% (100.0%)	97.5% (98.9%)
Refinement method	Full-matrix least-squares on F^2	Full-matrix least-squares on F^2	Full-matrix least-squares on F^2	Full-matrix least-squares on F^2
Data / restraints / parameters	1905 / 12 / 271	3196 / 1 / 272	2529 / 4 / 226	2162 / 55 / 227
Goodness-of-fit on F^2	1.080	1.016	1.065	1.014
Δ/σ_{max}	0.001	0.000	0.001	0.002
Final R indices [I>2σ(I)]	R_1 = 0.1150,	R_1 = 0.0665,	R_1 = 0.0691,	R_1 = 0.0733,
	wR_2 = 0.2979	wR_2 = 0.1645	wR_2 = 0.1693	wR_2 = 0.1554
R indices (all data)	R_1 = 0.1448,	R_1 = 0.1171,	R_1 = 0.1208,	R_1 = 0.1424,
	wR_2 = 0.3191	wR_2 = 0.1977	wR_2 = 0.2006	wR_2 = 0.1896
Flack x parameter	0.4(6)	0.0(2)	0.05(5)	0.00(13)
Largest diff. peak and hole (eÅ^{-3})	0.648 and -0.425	0.418 and -0.506	0.573 and -0.709	0.939 and -0.761
R.M.S. deviation from mean (eÅ^{-3})	0.095	0.063	0.111	0.138

$R_1 = \Sigma \; ||Fo|-|Fc|| \; / \; \Sigma \; |Fo|$

$wR_2 = \{\Sigma \; [w(Fo^2 - Fc^2)^2] \; / \; \Sigma \; [w(Fo^2)^2]\}^{½}$

Table 1bS. Hydrogen bonds geometrical parameters found in **Fmoc-4-F-Phe**, **Fmoc-4-Cl-Phe**, **Fmoc-4-Br-Phe** and **Fmoc-4-I-Phe** crystal packing.

Fmoc-4-F-Phe				
D-H···A	**d(D-H) (Å)**	**d(H···A) (Å)**	**d(D···A) (Å)**	**<(DHA)**
N(1)-HN1···O(3)#1	0.88	2.10	2.847(15)	142°
O(1)-H1···O(1S)	0.84	1.80	2.61(2)	161°
O(1)-H1···S(1S)	0.84	2.74	3.498(17)	151°
Symmetry transformations used to generate equivalent atoms: #1 x-1,y,z				

Fmoc-4-Cl-Phe				
D-H···A	**d(D-H) (Å)**	**d(H···A) (Å)**	**d(D···A) (Å)**	**<(DHA)**
O(1)-H(1A)...O(2)#1	0.84	1.81	2.645(11)	172°
N(1)-H(1)...O(3)#2	0.88	2.00	2.824(9)	156°
C(12)-H(12)...Cl(1)#3	1.00	2.87	3.516(9)	123°
Symmetry transformations used to generate equivalent atoms: #1 -x+2,y+1/2,-z+2 - #2 x,y+1,z - #3 -x+1,y+1/2,-z+1				

Fmoc-4-Br-Phe				
D-H···A	**d(D-H) (Å)**	**d(H···A) (Å)**	**d(D···A) (Å)**	**<(DHA)**
N(1)-HN1...O(3)#1	0.88	2.04	2.87(2)	155°
O(1)-H(1)...O(2)#2	0.84	1.76	2.58(2)	166°
Symmetry transformations used to generate equivalent atoms: #1 x,y,z+1 - #2 y,-x+y+1,z-1/2				

Fmoc-4-I-Phe				
D-H···A	**d(D-H) (Å)**	**d(H···A) (Å)**	**d(D···A) (Å)**	**<(DHA)**
N(1)-HN1...O(3)#1	0.88	2.09	2.90(4)	154°
O(1)-H(1)...O(2)#2	0.84	1.76	2.59(3)	170°
Symmetry transformations used to generate equivalent atoms: #1 x,y,z+1 - #2 y,-x+y+1,z-1/2				

Table 2S. Gelation properties of Fmoc-4-X-Phe.

AMINO ACID	AMINO ACID CONC.(mM)	DMSO PERCENTAGE	GELATION TIME	NOTES	Tgel-sol °C
FMOC-Phe	1.0	5%	/	Solution	n.d.
FMOC-4-F-Phe			/	Solution	n.d.
FMOC-4-Cl-Phe			30 min	Gel	59-66
FMOC-4-Br-Phe			10 min	Gel	69-73
FMOC-4-I-Phe			3 min	Gel	75-78
FMOC-Phe	2.5	5%	/	Solution	
FMOC-4-F-Phe			/	Solution	
FMOC-4-Cl-Phe			10 min	Gel	
FMOC-4-Br-Phe			1,5 min	Gel	
FMOC-4-I-Phe			1,5 min	Gel	
FMOC-Phe	5	5%	5 min	Gel	58-60
FMOC-4-F-Phe			5 min	Gel*	n.d.
FMOC-4-Cl-Phe			2 min	Gel	80-85
FMOC-4-Br-Phe			2 min	Gel	85-90
FMOC-4-I-Phe			1 min	Gel	95-105

* Poorly stable towards inversion

Table 3S. Minimum Gelation Concentration (MGC) for Fmoc-4-X-Phe in 5% DMSO/PBS.

AMINO ACID	MGC.(mM)
FMOC-Phe	5 mM
FMOC-4-F-Phe	3 mM*
FMOC-4-Cl-Phe	0.75mM
FMOC-4-Br-Phe	0.50mM
FMOC-4-I-Phe	0.25 mM

* Poorly stable towards inversion

Survey in the CCDC database.

Table 4S. Geometrical parameters set-up used to find in the CCDC database I···π interactions similar to the one found in Fmoc-4-I-Phe.

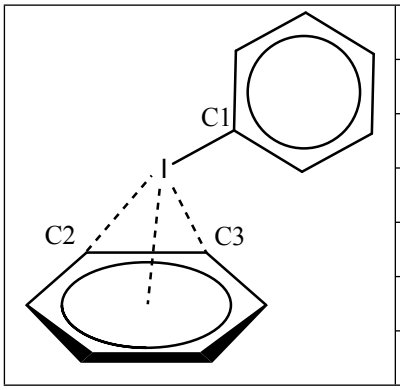

Parameter	Range
Distance I (I ··· Centroid)	0 4.68 Å
Distance II (I ··· C_2)	0 3.68 Å
Distance III (I ··· C_3)	0 3.68 Å
Angle I (C_1 I C_2)	0 180°
Angle II (C_1 I C_3)	0 180°
Angle III (C_1 I Centroid)	90 180°

Table 5S. Average values of the geometrical parameters of I···π interactions found in the CCDC database (299 hits) and comparison with Fmoc-4-I-Phe.

Parameter	Average	Fmoc-4-I-Phe
Distance I (I ··· Centroid)	3.69 Å	3.83 Å
Distance II (I ··· C_2)	3.54 Å	3.59 Å
Distance III (I ··· C_3)	3.54 Å	3.34 Å
Angle I (C_1 I C_2)	157.05°	169.87°
Angle II (C_1 I C_3)	158.60°	166.39°
Angle III (C_1 I Centroid)	156.35°	165.23°

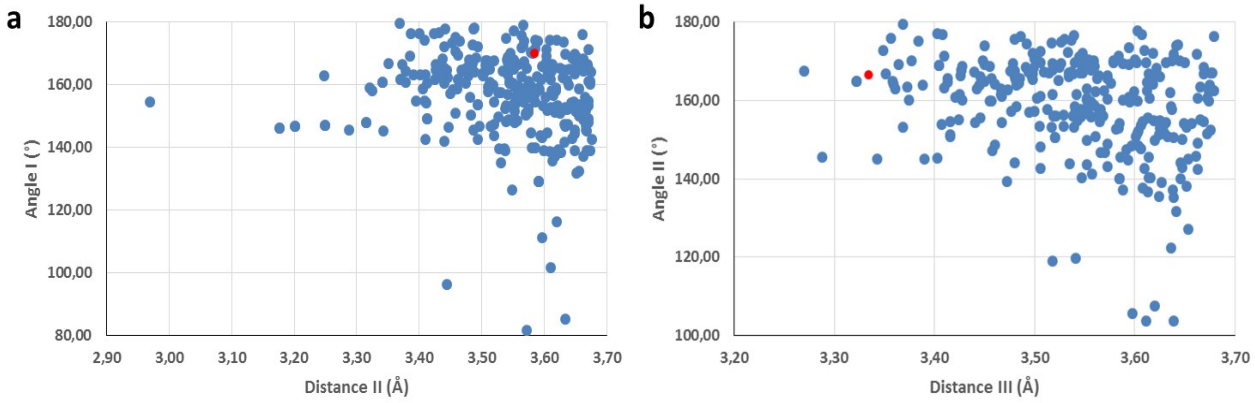

Figure 9S. a) Distance II plotted as a function of its corresponding angle. b) Distance III plotted as a function of its corresponding angle. The red spot is Fmoc-4-I-Phe.

Table 6S. Geometrical parameters set-up used to find in the CCDC database Br···π interactions similar to the one found in Fmoc-4-Br-Phe.

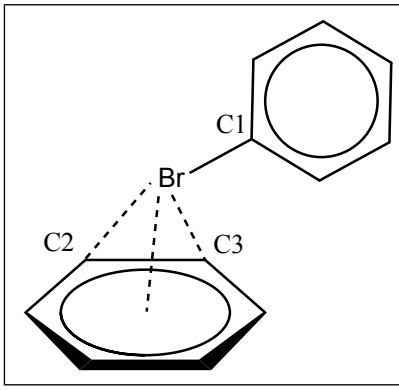

Parameter	Range
Distance I (Br···Centroid)	0 4.53 Å
Distance II (Br···C_2)	0 3.53 Å
Distance III (Br···C_3)	0 3.53 Å
Angle I (C_1 Br C_2)	0 180°
Angle II (C_1 Br C_3)	0 180°
Angle III (C_1 Br Centroid)	90 180°

Table 7S. Average values of the geometrical parameters of Br···π interactions found in the CCDC database (609 hits) and comparison with Fmoc-4-Br-Phe. Distance III and angle II are not reported for Fmoc-4-Br-Phe since in the crystal structure Bromine shows a contact with a unique carbon atom of the Fmoc moiety.

Parameter	Average	Fmoc-4-Br-Phe
Distance I (Br···Centroid)	3.64 Å	3.76 Å
Distance II (Br···C_2)	3.43 Å	3.26 Å
Distance III (Br···C_3)	3.42 Å	/
Angle I (C_1 Br C_2)	155.85°	167.95°
Angle II (C_1 Br C_3)	157.69°	/
Angle III (C_1 Br Centroid)	154.93°	164.19°

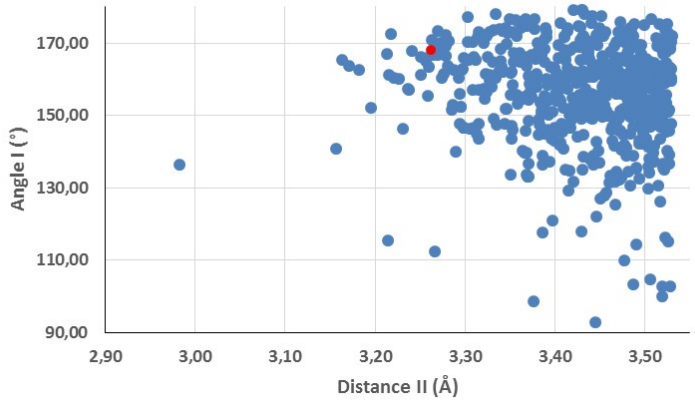

Figure 10S. Distance II plotted as a function of its corresponding angle. The red spot is Fmoc-4-Br-Phe.

References

[1S] S. R. Raghavan, B. H. Cipriano, Gel Formation: phase diagrams using tabletop rheology and calorimetry. In Molecular Gels, Materials with Self-Assembled Fibrillar Networks, R. G. Weiss, P. Terech Eds, Springer, Dordrecht, The Netherlands, 2006, 239-274.

[2S] Chuang-Chung Lee,* Arpan Nayak, Ananthakrishnan Sethuraman, Georges Belfort, and Gregory J. McRae, Biophys. J., 2007, 92, 3448-3458.

[3S] E. Giorgetti, P. Marsili, S. Cicchi, L. Lascialfari, M. Albiani, M. Severi, S. Caporali, M. Muniz-Miranda, A. Pistone, F. Giammanco, J. Colloid Interface Sci., 2015, 442, 89-96.

[4S] Lausi A., Polentarutti M., Onesti S., Plaisier J. R., Busetto E., Bais G., Barba L., Cassetta A., Campi G., Lamba D., Pifferi A., Mande S. C., Sarma D. D., Sharma S. M., Paolucci G., The European Physical Journal Plus, 2015, 130(43), 1-8.

[5S] Kabsch W. XDS. Acta Crystallographica Section D, 2010, 66(2), 125–132.

[6S] Winn, M. D., Ballard, C. C., Cowtan, K. D., Dodson, E. J., Emsley, P., Evans, P. R., Keegan, R. M., Krissinel, E. B., Leslie, A. G. W., McCoy, A., McNicholas, S. J., Murshudov, G. N., Pannu, N. S., Potterton, E. A., Powell, H. R., Read, R. J., Vagin, A. & Wilson, K. S., Acta Crystallographica Section D, 2011, 67, 235-242.

[7S] Evans P. R. and Murshudov G. N., Acta Crystallographica Section D, 2013, 69, 1204-1214

[8S] Zwart, P. H., Banumathi, S., Dauter, M. & Dauter, Z., Acta Crystallographica Section D, 2004, 60, 1958-1963.

[9S] McGeehan J. E., Carpentier P., Royant A., Bourgeois D., Ravelli R. B. G., Journal of Synchrotron Radiation, 2007, 14, 99-108.

[10S] Sheldrick G. M., Acta Crystallographica Section A, 2015, 71, 3-8.

[11S] Sheldrick G. M., Acta Crystallographica Section C, 2015, 71, 3-8.

[12S] Emsley P., Cowtan K., Acta Crystallographica Section D, 2004, 60(12), 2126–2132.

[13S] Parsons, S., Flack, H. D., Wagner, T., Acta Crystallographica Section B, 2013, 69(3), 249-259.

[14S] Farrugia, L., Journal of Applied Crystallography, 2012, 45(4), 849-854.

[15S] Macrae F., Bruno I. J., Chisholm J. A., Edgington P. R., McCabe P., Pidcock E., Rodriguez-Monge L., Taylor R., van de Streek J., Wood P. A., Journal of Applied Crystallography, 2008, 41, 466–470.